LONG RANGE TRANSPORT OF AIR POLLUTANTS

A cooperative OECD technical programme

SULPHUR TRANSPORT AND DRY DEPOSITION OVER EUROPE DESCRIBED BY A SIMPLE LAGRANGIAN DISPERSION MODEL

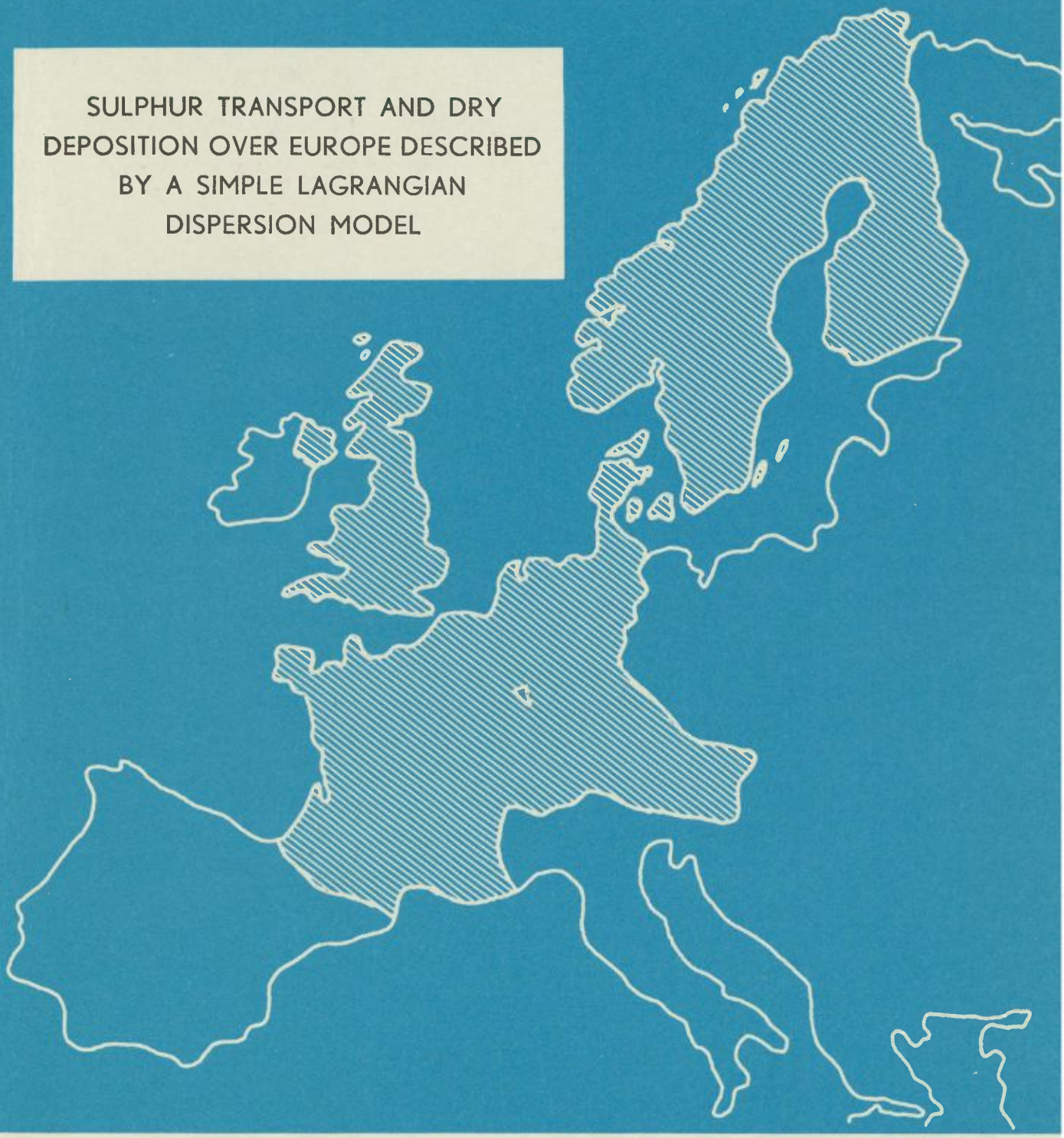

CENTRAL COORDINATING UNIT
Norwegian Institute for Air Research
P.B. 115 – 2007 Kjeller – Norway

LRTAP - 22/75
January 1976

SULPHUR TRANSPORT AND DRY DEPOSITION OVER EUROPE DESCRIBED BY A SIMPLE LAGRANGIAN DISPERSION MODEL

ANTON ELIASSEN AND JØRGEN SALTBONES

NORWEGIAN INSTITUTE FOR AIR RESEARCH
P.O. BOX 115, 2007 KJELLER
NORWAY

CONTENTS

ABSTRACT

A simple Lagrangian dispersion model is described and applied to sulphur pollution over Europe. The model calculations are based on available SO_2-emission data for Europe, and wind observations in the 850 mb surface. A special case is reported where the presence of computed large-scale SO_2 and SO_4 plumes are verified by concentration data from aircraft sampling and from the LRTAP sampling network. For stations in this network, computed and observed daily mean SO_2 and SO_4 concentrations are compared for a period of six months. Based on this comparison SO_2 dry deposition patterns for Europe are calculated, using computed mean concentrations and a deposition velocity of 0.8 cms^{-1}.

1 INTRODUCTION

As part of the OECD-project "Long Range Transport of Air Pollutants" (LRTAP) a network of sampling stations have been set up in the participating countries. The data obtained from this network are daily mean concentrations of chemical components in precipitation and air. Two components in air are measured: SO_2 and particulate SO_4. Surveys of anthropogenic SO_2-emission within Europe have been carried out in connection with the project. Atmospheric dispersion models have been developed to link the emission surveys and the observed concentrations.

In the following a simple Lagrangian-type dispersion model is described. The model includes a transformation $SO_2 \rightarrow SO_4$ and thus gives estimates of SO_2 and SO_4 air concentrations. As an example the model calculations are compared with observed concentrations in a situation with large-scale SO_2 and SO_4 plumes crossing the North Sea. In this case the data from the LRTAP sampling network are completed with concentrations measured from the NILU aircraft. In addition, calculated concentrations are compared with observations from the LRTAP network for a period of six months starting from December 15, 1973. Based on this comparison a SO_2 dry deposition pattern for Europe 1974 is calculated, using computed mean concentrations and a deposition velocity of 0.8 cms^{-1}.

2 THE DATA

The SO_2-emission data used in this work are based on available information from the United Nations Economic Commission for Europe, and from OECD's Air Management Sector Group. A grid map giving the figures have been published elsewhere (Eliassen and Saltbones 1975). Better information has now been received for most of the countries, but a complete survey was not available for this investigation. The yearly emission

data are believed to be within ±20% of the actual figures, but may be somewhat more uncertain for the Eastern European countries. No seasonal variation has been included in the emission figures.

The air concentration measurements within the LRTAP network are carried out by laboratories in the participating countries, using sampling and analysis methods specified for the project. The detection limits have been estimated to 2-5 μgm^{-3} for SO_2, and better than 1 μgm^{-3} for particulate SO_4. Locations of the sites used in this investigation are shown in Figure 2. The geographical coordinates of the sites used in the six months comparison with model calculations, are given in Table 2.

The wind fields used for advection are based on wind observations in the 850 mb surface at 00, 06, 12 and 18 GMT. To obtain gridpoint values, the two wind components are analysed independently. The time interpolation between observation hours is linear in each component.

3 DESCRIPTION OF THE MODEL

Consider a layer of air of thickness h flowing horizontally over a flat surface. Assume that the SO_2 and SO_4 are completely mixed up to the height h, that the wind does not change with height and that the air has a constant density. The equations of continuity for SO_2 and SO_4 within the layer are

$$\frac{Dq}{dt} = E_q - F_q \qquad (1)$$

$$\frac{Ds}{dt} = E_s - F_s \qquad (2)$$

where q and s are the concentrations of SO_2 and SO_4, and E_q, E_s, F_q, F_s are source and sink terms for SO_2 and SO_4. The operator D/dt denotes the total time derivative along a trajectory. The quantities in equations (1) and (2) are independent of the vertical coordinate.

The SO_2-emission term E_q is equal to Q/h, where Q is the SO_2-emission per unit area and time at the current position of the trajectory, taken from the emission inventory referred to earlier. For this work, the emission map used earlier has been transformed to another grid and extended somewhat towards the east. Both grids have a grid distance of 127 km at 60°N. No attempts is made to describe in detail the various transformation and removal processes of SO_2. The transformation $SO_2 \rightarrow SO_4$ is assumed to be of first order, and the removal rates of SO_2 and SO_4 are assumed to be proportional to the concentrations. With these assumptions the equations (1) and (2) become

$$\frac{Dq}{dt} = \frac{Q}{h} - kq \qquad (3)$$

$$\frac{Ds}{dt} = \frac{3}{2} k_t q - \kappa s \qquad (4)$$

k_t is the transformation rate for $SO_2 \rightarrow SO_4$, and k, κ are removal rates for SO_2 and SO_4. The factor 3/2 is the ratio of molecular weights of SO_4 and SO_2. The following values were used for the constants:

$$k = 10^{-5}\ s^{-1}$$
$$k_t = \kappa = 10^{-6}\ s^{-1}$$
$$h = 10^3 m$$

The authors have earlier (Eliassen and Saltbones, 1975) reported some estimates of k and k_t using a method based on

trajectories arriving at LRTAP sampling sites. These estimates were on the average about twice as large as the values given above. When complete vertical mixing of SO_2 up to the height h is assumed, a deposition velocity $v_s = 1\ cms^{-1}$ gives a removal rate $v_s/h = 10^{-5}s^{-1}$.

In the model, isobaric trajectories for marked particles are computed using the observed and analysed 850 mb winds. The SO_2 and SO_4 concentrations q and s associated with the marked particles change according to equations (3) and (4). At the start of the integration, the number of marked particles is equal to the number of emission squares (32 x 32), and each marked particle is positioned in the middle of an emission square. New positions for the particles are calculated every $\Delta t = 1$ hr, using a method described by Petterssen (1956).

Every 12 hours, 00 and 12 GMT, the integration is restarted with new marked particles in the middle of the emission squares. By this time, about 15% of the old particles have disappeared across the grid boundary. The SO_2 and SO_4 concentrations of the new particles are obtained from those of the remaining old particles by a simple interpolation procedure: A new particle is given the mean concentration of the old particles present in its grid element. If no old particles are present there, a time interpolation is carried out, using the concentrations of old particles at the preceding and the next timesteps. The small number of new particles which have not received a concentration by either of these procedures, are given the mean concentrations of the old particles in the neighbouring grid elements. By this procedure, the number of marked particles with non-zero concentrations may be slightly different before and after the interpolation, depending on how uniformly the old particles are distributed in the grid. In the calculations presented here, the sums of concentrations associated with the particles before and after interpolation differ by typically ±3%.

Figure 1 shows the result of a model integration in a rotating wind field with a constant angular velocity, starting with zero concentrations everywhere. Emissions are zero everywhere except for a block of six grid elements with emissions of equal strength. One timestep in the integration corresponds to a rotation of 2.3 degrees, or a movement of about 1/3 of a gridlength for particles crossing the emission block. The integration is restarted every 55 degrees of rotation, using the interpolation procedure described above. Figure 1 shows the concentration field after a rotation of 110 degrees and 2 restarts of the integration. It is seen that the truncation errors are generally confined to neighbour grid elements in the final presentation.

Model estimates of daily mean SO_2 and SO_4 concentrations at a sampling site are obtained by averaging the estimated concentrations of the timesteps covering one day. The concentration estimate at a certain timestep is the mean value of the concentrations associated with the particles present inside a circle around the sampling site with the same area as an emission square. If no particles are present inside the circle, the concentration estimate of the previous timestep is used.

4 COMPUTED LARGE-SCALE SO_2 AND SO_4 PLUMES VERIFIED BY CONCENTRATION MEASUREMENTS FROM AIRCRAFT

As part of the LRTAP programme a number of concentration measurements from aircraft have been carried out. The measured concentrations are horizontal averages at a certain height, typically over a distance of about 100 km, corresponding to a sampling time of about 30 minutes. Due to the large instantaneous concentration gradients which especially occur near large sulphur emissions, the concentrations measured from aircraft are not directly comparable to calculated concentrations. The aircraft measurements may, however, confirm the existence of large-scale SO_2 and SO_4 plumes implied by the model calculations. Such a case is shown in Figures 3 and 4.

The figures show the computed SO_2 and SO_4 concentration fields at 12 GMT May 10, 1974. A low pressure cell approaching from the west has set up a southeasterly airflow across the North Sea. The concentration measurements made with the NILU aircraft are shown on the figures, together with daily mean concentrations from the ground sampling sites of the LRTAP programme. The flight height was around 550 m.

The figures show that in this case, the model gives about the right concentration levels of SO_2 and SO_4, both when comparing with aircraft measurements and the observations from the ground sampling sites. Generally, there is a variable agreement between the concentrations measured at the surface and the aircraft measurements, due to vertical concentration gradients.

The observations confirm the existence of the computed SO_2 and SO_4 plumes 500 km away from the closest upwind anthropogenic sulphur emissions. Possibly a slight displacement of the computed plumes towards the left would fit the aircraft measurements better. This is consistent with barotropic boundary layer theory since the sampling height is well below the 850 mb surface, where the winds used for advection are observed.

5 MODEL ESTIMATES COMPARED TO OBSERVED SO_2 AND SO_4 AIR CONCENTRATIONS AT LRTAP SAMPLING SITES

Model calculations have been carried out for a period of more than three years, starting from July 1, 1972. The model estimates are compared with observed concentrations from the LRTAP ground sampling network for a period of six months, starting from December 15, 1973. The set of observed concentrations from this period is fairly complete, and the data are considered more reliable than data from earlier periods.

In Table 1, the computed and observed six-monthly mean values of SO_2 and SO_4 air concentrations at 29 LRTAP sampling sites are listed. The table also gives the correlation coefficients between observed and computed daily concentrations in the period. For most sampling sites the number of daily concentration pairs were between 180 and 170, except for D2, D3, DK4 where the numbers were around 160, and DK6, NL4 where they were around 150. The SO_4 correlation coefficients range from 0.241 to 0.775. The corresponding coefficients for SO_2 range from -0.019 to 0.610. At all sampling sites except two, the SO_4 correlation coefficients are higher than the SO_2 coefficients, even though the transformation $SO_2 \rightarrow SO_4$ is described simply as a first order reaction in the model. Some explanation for this may be provided by the frequency distribution of observed and computed daily concentrations. At the site UK1 for example, (Figure 5) SO_2 concentrations lower than 16 μgm^{-3} are much more often observed than computed. The model, in which complete mixing in a grid volume is assumed, is unable to explain the observed low SO_2-concentrations in areas with large emissions. In these areas, the SO_2 is far from being uniformly distributed within a grid volume, because a significant part of it is emitted from point sources. For the SO_4, the mean transformation rate is slow enough to allow time for a more thorough mixing. Therefore, SO_4 is more uniformly distributed in the atmosphere than SO_2, and behaves more according to the model assumptions.

Factors like wet deposition, vertical concentration gradients and wind shear are not included in this simple advection model. This limits the day-to-day agreement obtainable between observations and model estimates.

6 ESTIMATED SO_2 DRY DEPOSITION PATTERNS

Figures 6 and 7 show the computed six-monthly mean concentrations plotted against the observed ones (data in Table 1). Denoting the observed and computed SO_2 six-monthly mean concentrations by y and x respectively, the linear regression line of y on x is:

$$y = 0.604\ x + 1.85\ \mu gm^{-3} \qquad (5)$$

with a correlation coefficient of 0.935. Assuming random sampling from normal populations, the 99% confidence limits for the regression coefficient are 0.603 ± 0.125. From Figure 6 it is seen that the ratio between observed and computed mean concentrations decreases moderately from sites with low mean concentrations to sites with higher ones. Since the SO_2 present at the sites with small mean values has a longer mean transport time than sites with high values, this indicates that the mean decay rate of $10^{-5}s^{-1}$ for SO_2 employed in the calculations is fairly close to the true value. The mean transport time for SO_2 to the various sites is known only very roughly, from the available data it may only be concluded that the decay rate employed should be correct within a factor of 2.

The correspondence between computed and observed SO_4 six-monthly mean values is not as good (Figure 7), even though the day-to-day correlation is better than for SO_2. Evidently, the low mean values are overestimated and high ones underestimated. A larger value of κ in equation (4) would better this situation, as this would reduce the low computed values relatively more than the high ones. The overall SO_4 concentration level can be adjusted by means of the transformation rate k_t.

The good correspondence between computed and observed six-monthly mean SO_2 concentrations encourages a calculation of SO_2 dry deposition patterns for Europe. Six-monthly mean concentrations of SO_2 for each emission square is calculated from the model concentrations at 00 and 12 GMT each day. To transform these to ground level concentrations, the computed values are adjusted by means of the line $y = 0.719\ x$, instead of using the linear regression line (5). Both lines are shown on Figure 6. To obtain the dry deposition flux, a deposition velocity of 0.8 cms^{-1} is employed, a value estimated by Owers and Powell (1974) to be representative for the British Isles (referred to concentrations measured 20 cm over the surface). Garland et al. (1974) and Shepherd (1974) also report deposition velocities of about the same magnitude for grass and water surfaces, for situations with friction velocities larger than about 0.3 ms^{-1}.

The resulting SO_2 dry deposition patterns for six periods of six months are shown on Figures 8-13. Since a constant deposition velocity of $8 \cdot 10^{-3} ms^{-1}$ has been employed, the Figures may just as well be regarded as mean concentration patterns, a six-monthly dry deposition of 1 g SO_2 m^{-2} corresponding to a mean concentration of 8 μgm^{-3}.

The calculated deposition patterns vary little from one period to another. The small differences between the patterns are due only to differences in the observed wind fields.

The LRTAP sampling sites were placed well away from major emissions so that the concentration data would reflect the large scale concentration field. The measured concentrations may therefore be an underestimate for the average ground level concentration in a grid element, and consequently the estimated dry deposition in areas with large emissions may be too small.

The importance of this effect depends upon the distribution of the ground level concentration inside the grid elements. Information on such distributions are not readily available, thus the evaluation of this effect would require extensive additional investigation on the sub-grid scale, taking into consideration that a significant part of the emissions are warm emissions from tall stacks, and that urban plumes may be lifted from the surface by thermal effects.

Bolin and Persson (1975) have presented similar dry deposition patterns, using a statistical formulation of the continuity or transport equation. The horizontal dispersion of sulphur was calculated using the statistical properties of a large number of trajectories initiated every third day from five different points in Europe. The vertical dispersion was treated by an eddy diffusion approach, using a mean emission height of 85 m, and a constant deposition velocity at the roughness height z_0 as the lower boundary condition.

The shape of the dry deposition patterns of Bolin and Persson agree fairly well with the patterns presented in this work. However, the patterns of Bolin and Persson show smaller deposition values far away from the areas with large emissions, reflecting a shorter residence time of sulphur in the atmospheric boundary layer.

REFERENCES

Bolin, B. and Persson, C. 1975. Regional dispersion and deposition of atmospheric pollutants with particular application to sulfur pollution over Western Europe.
Tellus 27, 281-310.

Eliassen, Anton and Saltbones, Jørgen. 1975. Decay and transformation rates of SO_2 as estimated from emission data, trajectories and measured air concentrations.
Atmospheric Environment 9, 425-429.

Garland, J.A., Atkins, D.H.F., Readings, C.J. and Caughey, S.J. 1974. Deposition of gaseous sulphur dioxide to the ground.
Atmospheric Environment 8, 75-79.

Owers, M.J. and Powell, A.W. 1974. Deposition velocity of sulphur dioxide on land and water using a ^{35}S tracer method.
Atmospheric Environment 8, 63-67.

Petterssen, S. 1956.
Weather analysis and forecasting, McGraw-Hill, p 27.

Shepherd, J.G. 1974. Measurements of the direct deposition of sulphur dioxide onto grass and water surfaces by the profile method.
Atmospheric Environment 8, 69-74.

	SO_2			SO_4			Geographic coordinates of sampling sites		
	Mean concentrations		Correlation	Mean concentrations		Correlation			
	Observed	Computed	Coefficient	Observed	Computed	Coefficient	N Lat	Longitude	Altitude (m)
D 2	25.8	39.8	0.194	5.2	7.2	0.241	52 48	10 45 E	73
D 3	14.6	22.9	0.033	3.9	7.5	0.354	47 58	7 57 E	1200
DK1	-	-	-	0.5	2.8	0.359	62 04	6 58 W	740
DK2	7.5	10.1	0.141	6.3	4.9	0.656	57 07	8 36 E	46
DK3	7.4	14.1	0.086	7.9	5.2	0.498	56 21	9 36 E	13
DK4	11.3	17.5	-0.006	6.8	5.2	0.447	56 00	11 17 E	3
DK5	9.2	19.2	0.321	8.0	5.8	0.484	54 44	10 44 E	8
DK6	10.3	16.9	-0.019	9.3	5.7	0.245	55 00	15 05 E	6
F 1	24.7	26.2	0.609	17.7	6.2	0.775	48 32	2 22 E	64
N 1	8.1	8.3	0.495	5.1	4.4	0.627	58 23	8 15 E	190
N 3	5.6	7.7	0.310	4.6	4.4	0.588	58 19	7 35 E	275
N 9	5.8	6.9	0.386	4.5	4.2	0.532	58 41	5 59 E	263
N22	11.5	9.4	0.229	7.0	4.2	0.489	59 04	10 26 E	35
N23	7.9	8.9	0.264	5.4	4.3	0.419	58 38	9 08 E	20
N25	3.3	3.7	0.564	1.7	3.4	0.669	62 27	11 16 E	1539
NL1	24.3	38.2	0.346	12.1	6.6	0.564	51 58	5 38 E	7
NL2	17.7	31.9	0.547	8.5	6.1	0.636	52 49	6 40 E	17
NL3	14.3	26.9	0.327	8.9	6.1	0.580	52 55	4 47 E	0
NL4*	31.5	38.6	0.568	11.0	6.6	0.661	51 28	5 29 E	29
S 3	6.2	10.0	0.444	5.3	4.1	0.501	58 46	14 18 E	125
S 4	5.1	7.8	0.030	5.5	3.8	0.495	59 46	17 05 E	30
S 5	3.1	3.2	0.194	2.7	3.0	0.435	63 51	15 17 E	405
SF1	6.5	6.9	0.284	2.2	3.7	0.479	60 11	19 59 E	15
SF2	5.2	7.9	0.242	2.4	3.6	0.363	60 49	23 30 E	104
SF3	10.5	6.6	0.486	2.9	3.5	0.390	61 34	28 04 E	120
SF4	5.8	4.4	0.498	1.9	3.3	0.427	62 31	24 13 E	154
SF5	5.1	1.8	0.318	1.4	2.6	0.340	67 22	26 39 E	178
UK1	23.4	37.0	0.236	7.7	5.3	0.700	51 58	0 06 W	125
UK2	12.7	18.4	0.610	6.0	5.0	0.689	55 19	3 12 W	236

* The estimates are those of NL1, but fewer cases.

Table 1: Computed and observed six-months mean concentrations at LRTAP sampling sites. Also given are the correlation coefficients between computed and observed daily SO_2 and SO_4 concentrations in the same period, starting December 15, 1973. In addition the geographic coordinates of the sampling sites are listed. All concentrations are in μgm^{-3} as SO_2 or SO_4.

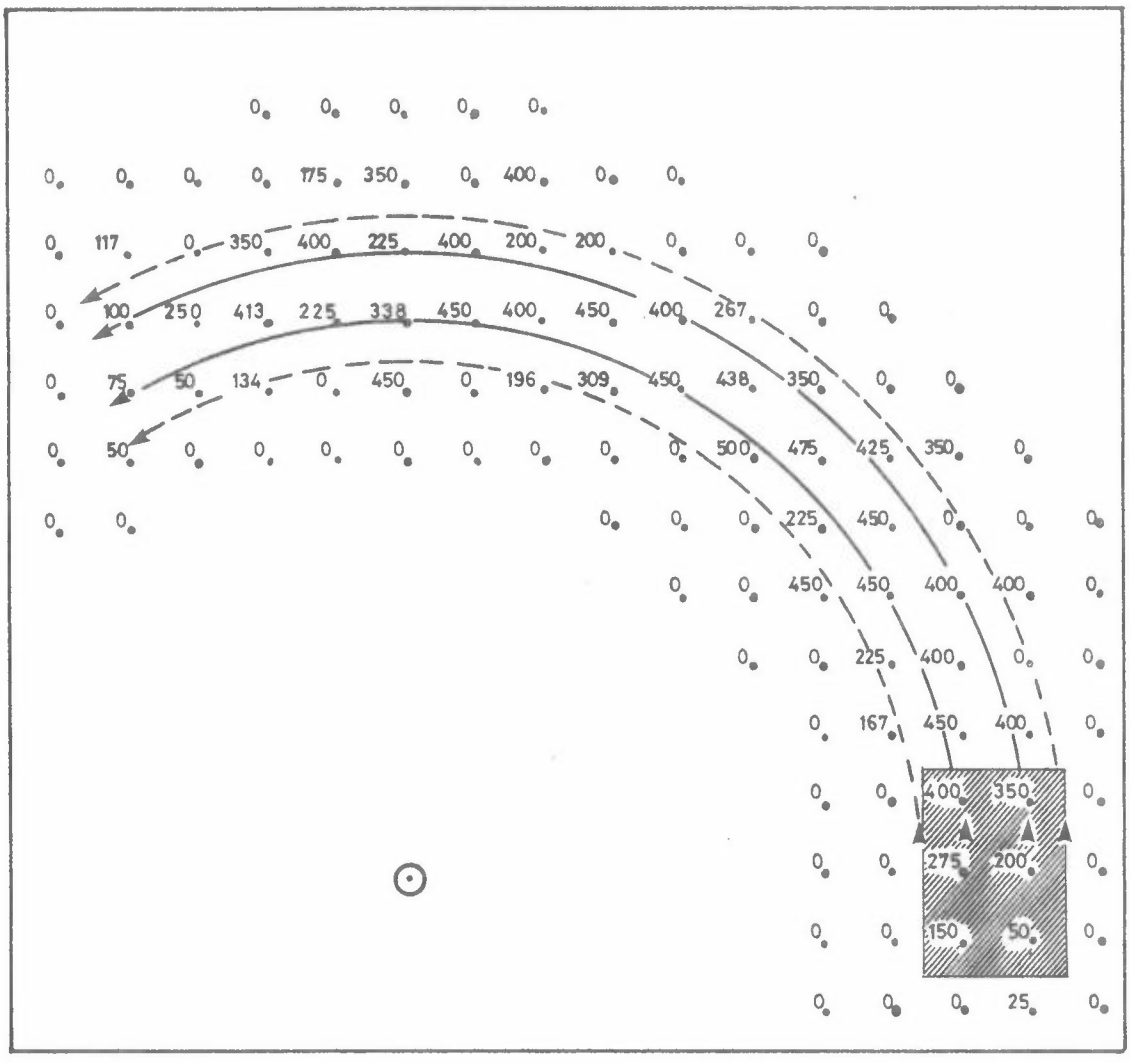

Figure 1: Result of model integration in a rotating wind field with a constant angular velocity, starting with zero concentrations everywhere. Emissions are zero everywhere except for a block of six grid elements with emissions of equal strength. The figure shows the concentration field after 48 timesteps and 110 degrees of rotation, with interpolation at 55 and 110 degrees (see text).

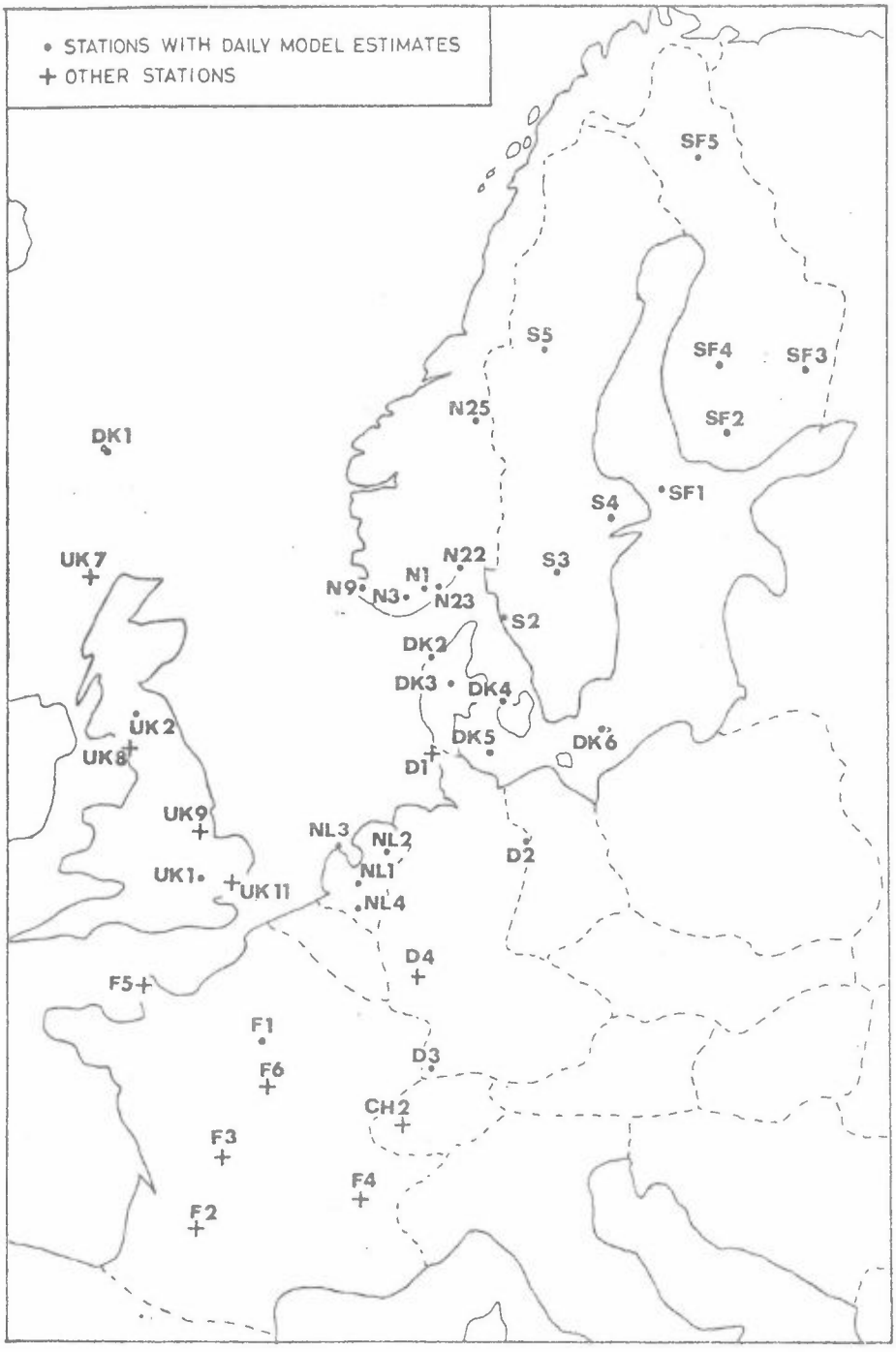

Figure 2: Location of LRTAP sampling sites providing data for this investigation. Data from stations marked with + appear only on Figures 3 and 4.

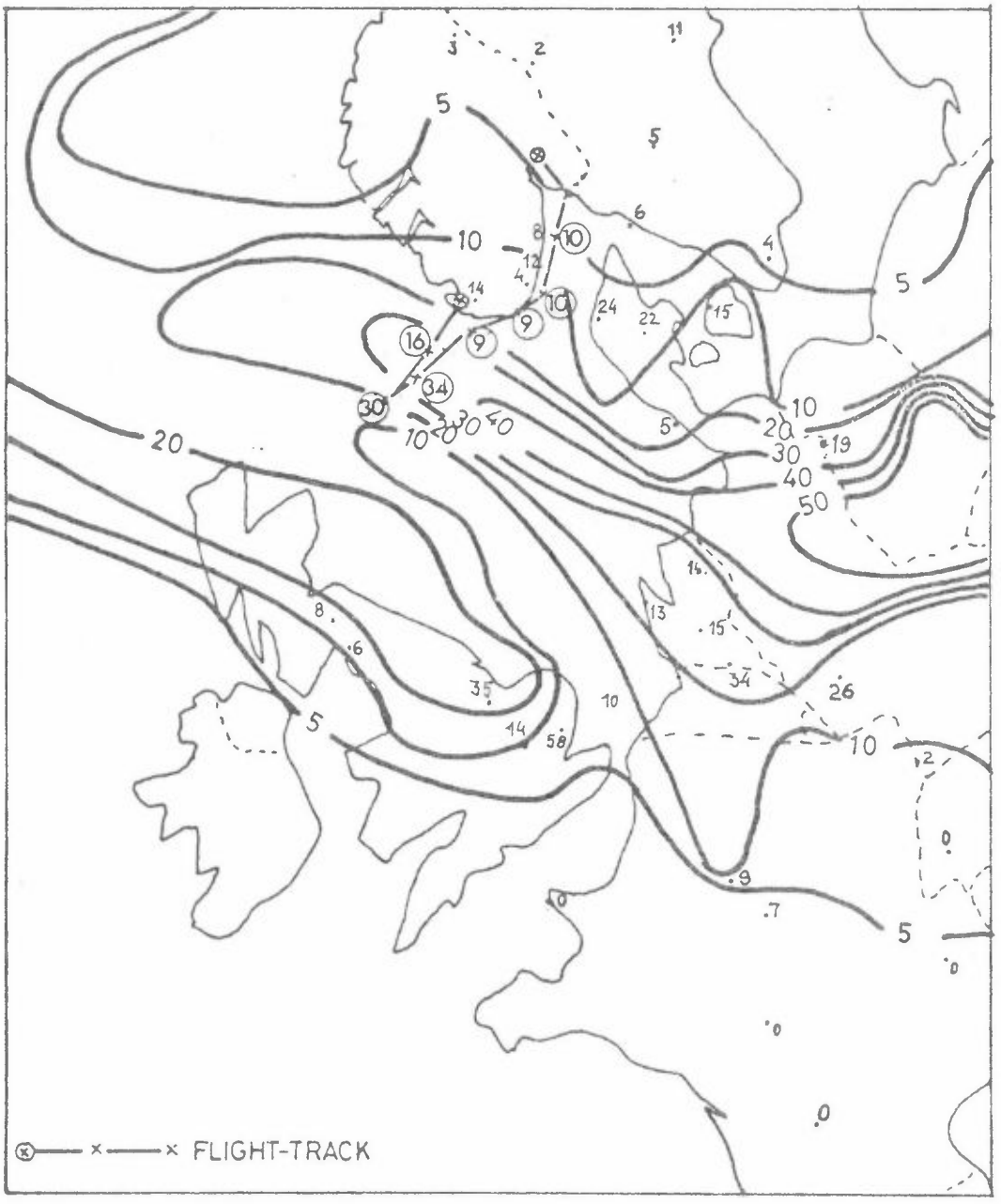

Figure 3: Computed SO_2-concentrations at 12 GMT May 10, 1974, (isolines) together with aircraft measurements (in circles) and daily mean concentrations from the LRTAP-network.
Unit: µg SO_2/m^3.

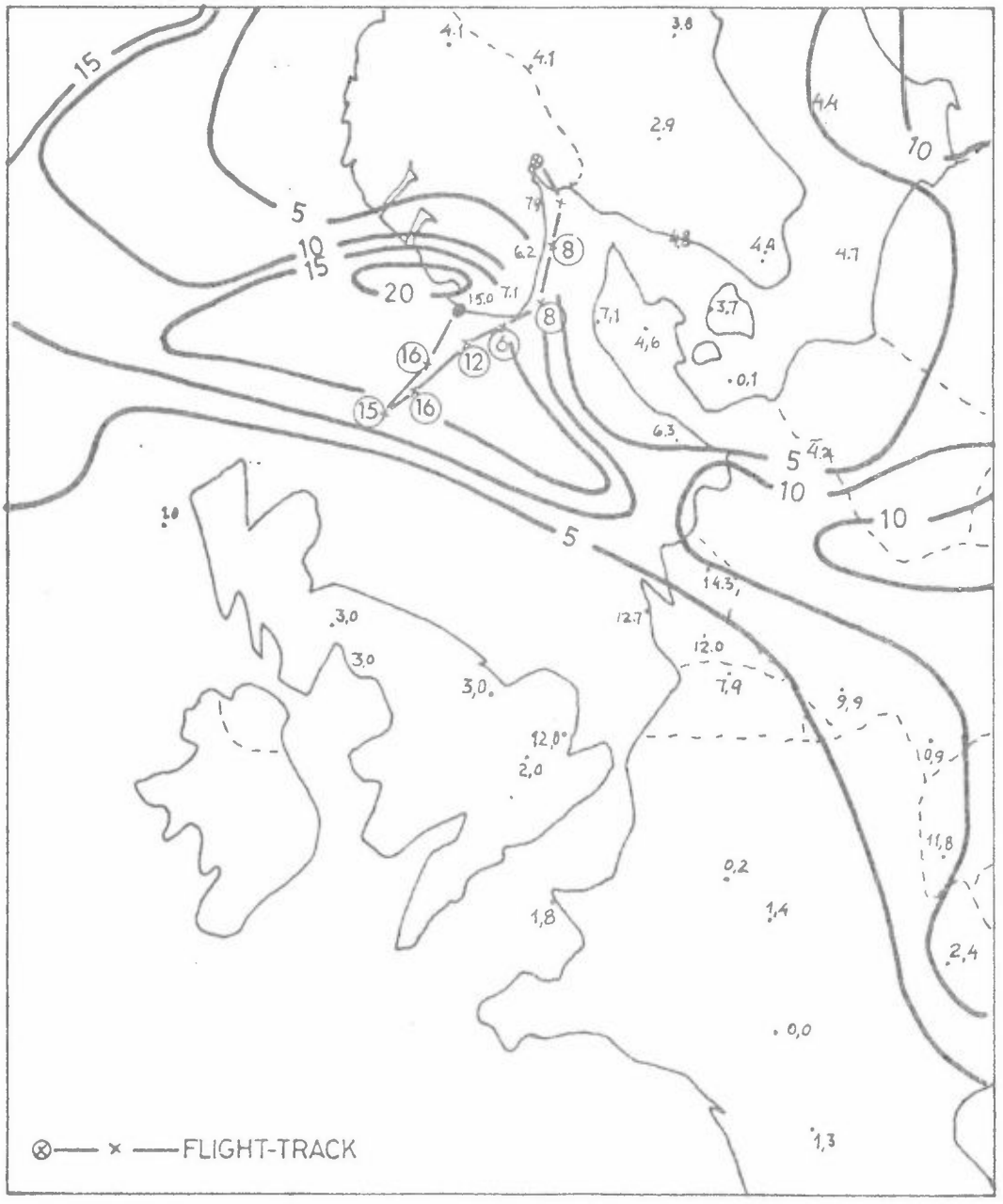

Figure 4: Computed SO_4-concentrations at 12 GMT May 10, 1974, (isolines) together with aircraft measurements (in circles) and daily mean concentrations from the LRTAP-network.
Unit: µg SO_4/m^3.

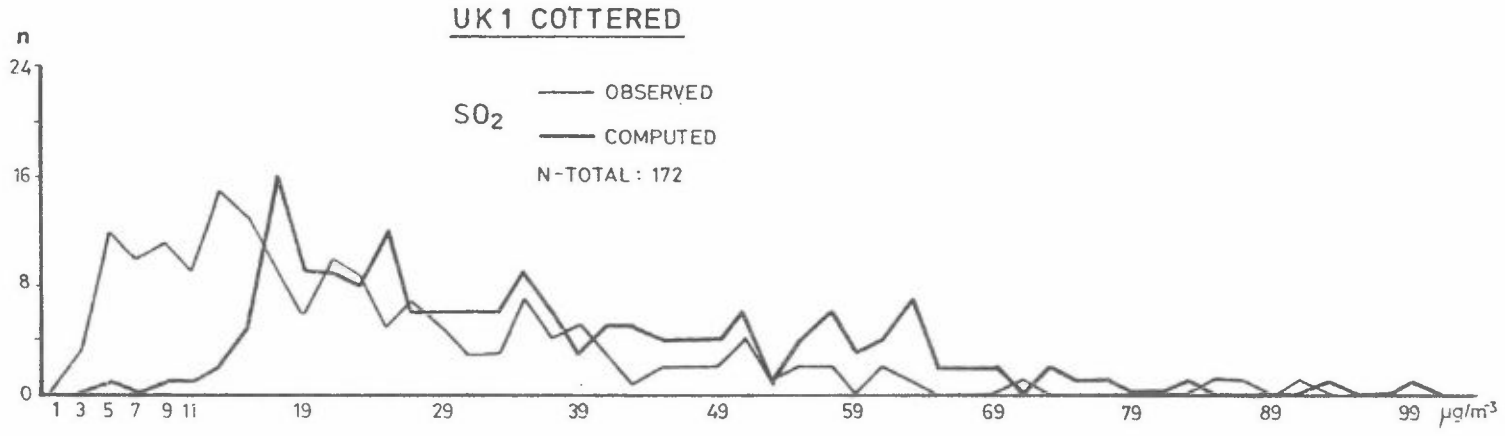

Figure 5: Frequency distribution of observed and computed daily mean SO_2-concentrations at the site UK1.

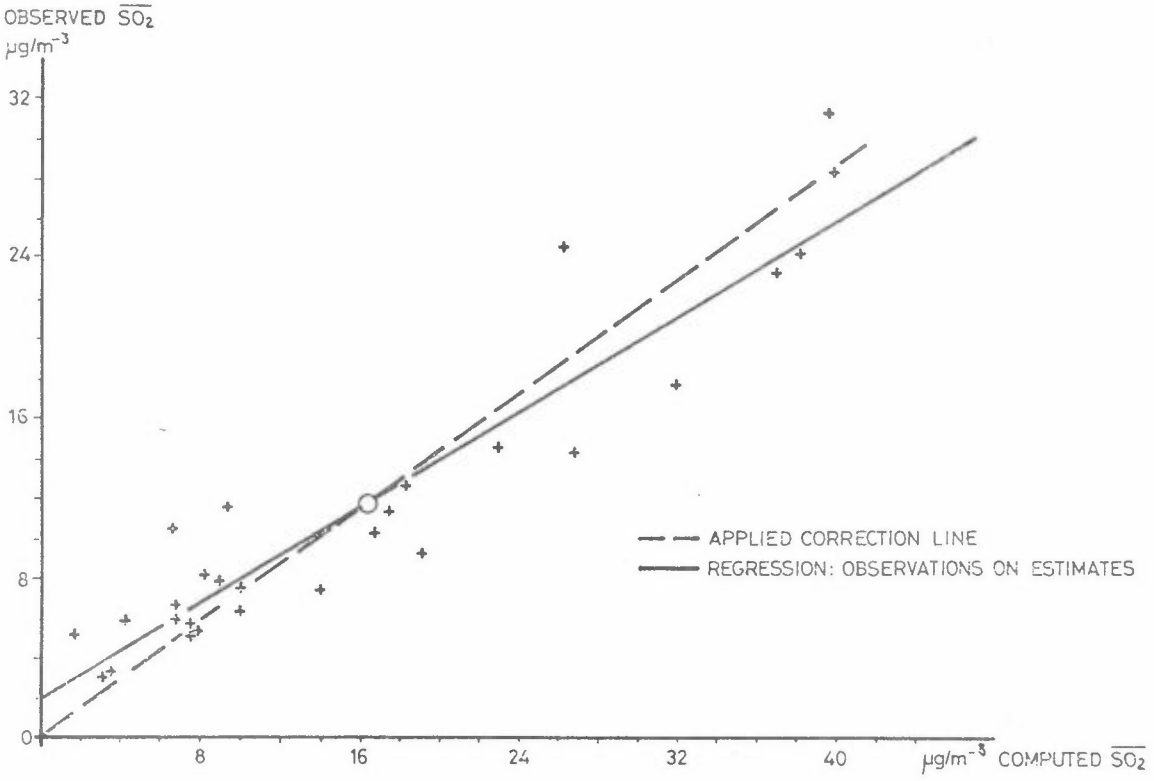

Figure 6: Computed six-monthly mean SO_2-concentrations plotted against observed ones. The linear regression line of observations on estimates is shown together with correction applied when calculating dry deposition.

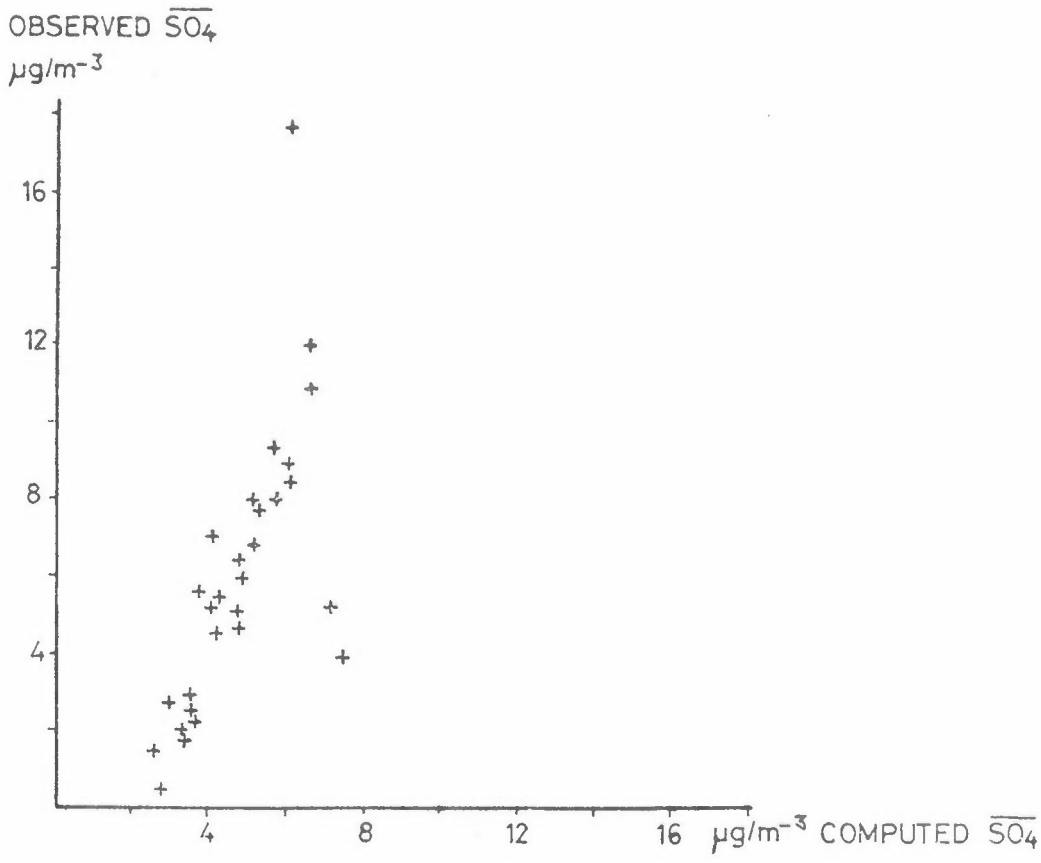

Figure 7: Computed six-monthly mean SO_4-concentrations plotted against observed ones.

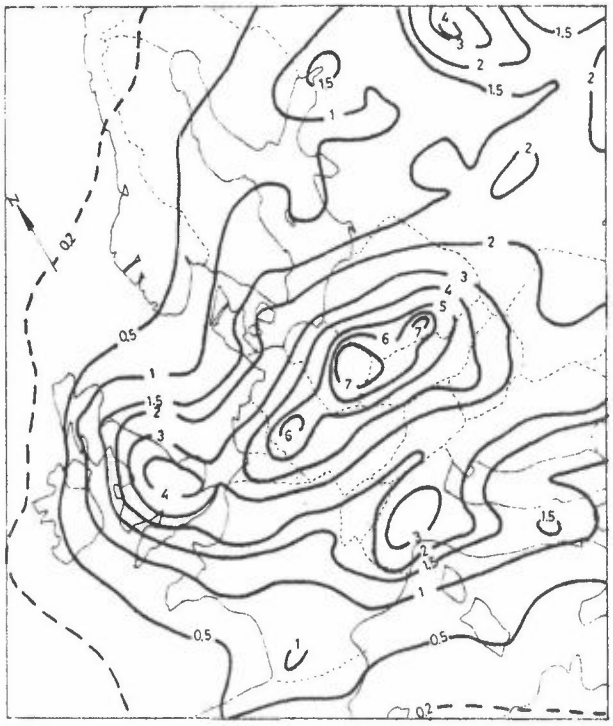

Figure 8: Calculated SO_2 dry deposition pattern for the second half of 1972.
Unit: g $SO_2 m^{-2}$.

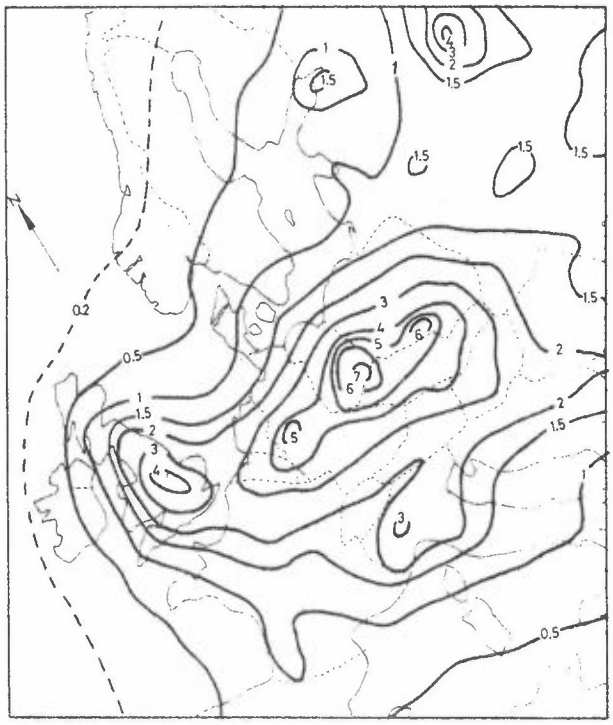

Figure 9: Same as Figure 8, but for first half of 1973.

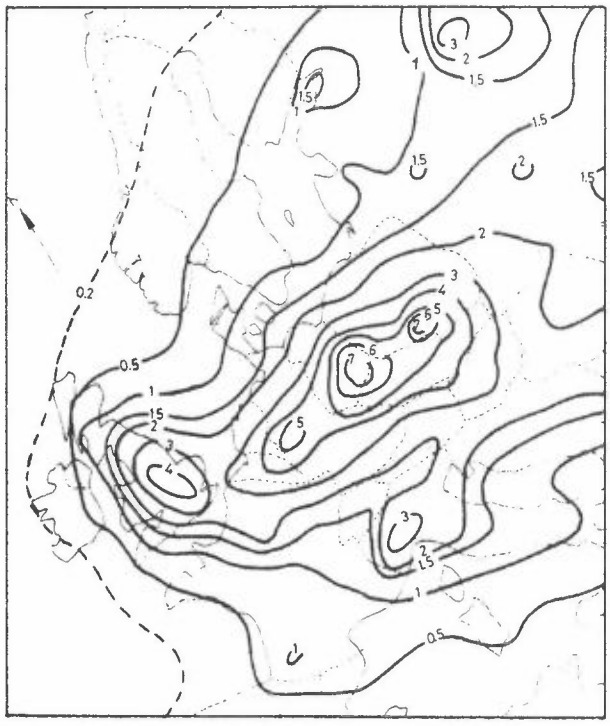

Figure 10: Same as Figure 8, but for second half of 1973.

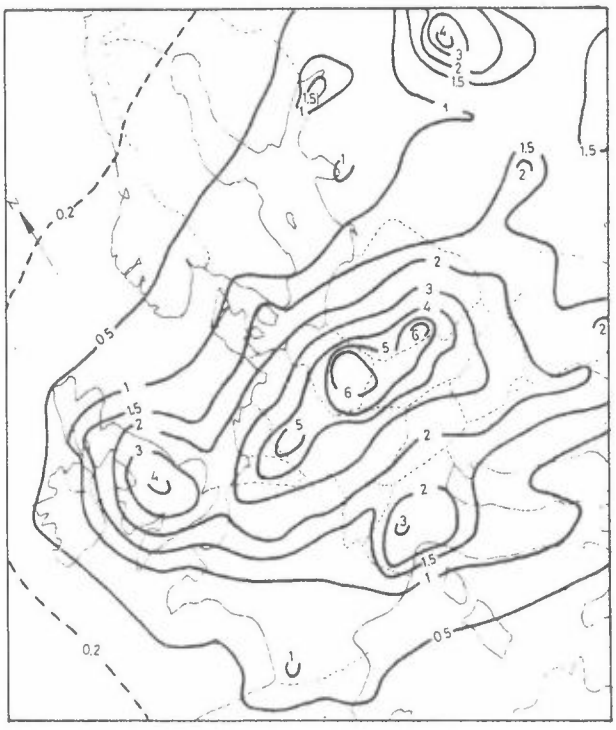

Figure 11: Same as Figure 8, but for first half of 1974.

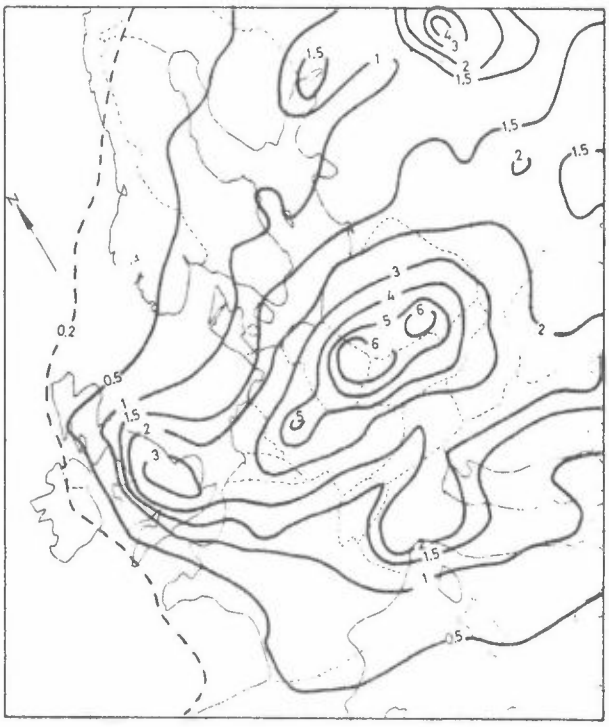

Figure 12: Same as Figure 8, but for second half of 1974.

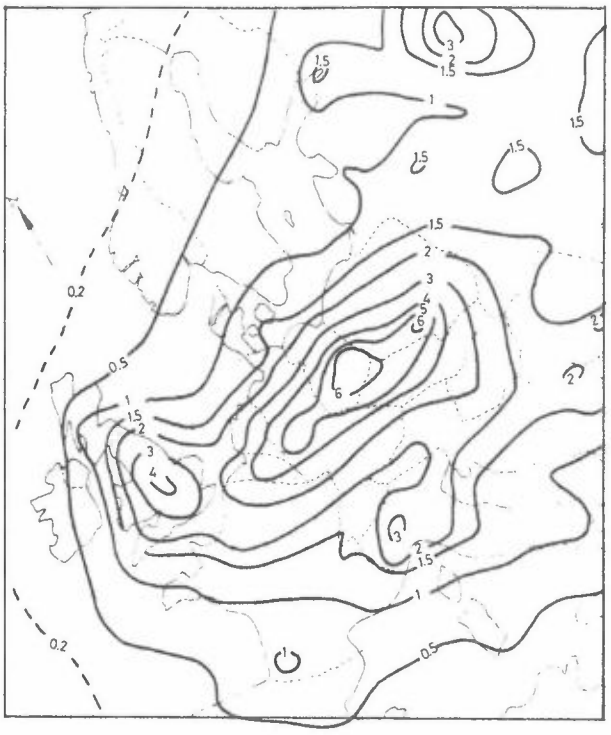

Figure 13: Same as Figure 8, but for first half of 1975.